Oblique terahertz plasmons in graphene nanoribbon arrays

doi: 10.1103/PhysRevB.81.073404

Oblique terahertz plasmons in graphene nanoribbon arrays

V. V. Popov,[1,2] T. Yu. Bagaeva,[1] T. Otsuji,[2,3] and V. Ryzhii[4,3]
[1]*Kotelnikov Institute of Radio Engineering and Electronics, Saratov 410019, Russia*
[2]*Research Institute of Electrical Communication, Tohoku University, Sendai 980-8577, Japan*
[3]*CREST, Japan Science and Technology Agency, Tokyo 107-0075, Japan*
[4]*Computational Nanoelectronics Laboratory, University of Aizu, Aizu-Wakamatsu 965-8580, Japan*
(Received 8 October 2009; published 9 February 2010)

We show that the plasmon frequencies in a one-dimensional dense array of doped (or gated) graphene nanoribbons can be changed through the entire terahertz range depending on the angle between the plasmon wave vector and the nanoribbon direction. The overdamped regime for oblique plasmons in the graphene nanoribbon array is discussed.

DOI: 10.1103/PhysRevB.81.073404 PACS number(s): 73.20.Mf, 78.67.−n, 81.05.U−

Graphene, a two-dimensional (2D) monolayer of graphite has received a great deal of interest recently due to its unique electronic properties stemming from a linear (Dirac-type) gapless carrier energy spectrum in graphene $E=\pm V_F|\mathbf{p}|$, where E and $\mathbf{p}$ are the electron (hole) energy and momentum, respectively, and $V_F\approx 10^8$ cm/s is a band parameter (the 2D Fermi velocity, which is a constant for graphene), and upper and lower signs refer to the conduction and valence bands, respectively.[1–5] Plasmons in intrinsic and doped graphene have been investigated lately.[6–11] The plasmon frequency is proportional to the square root of the plasmon wave vector for ungated graphene[7,9,10] and varies lineary with the plasmon wave vector for gated graphene[6,11] similar to plasmons in conventional (mostly semiconductor based) 2D electron systems (see, e.g., Ref. 12, and references therein). This is a consequence of general properties of the long-range Coulomb interaction defining the plasmon frequency in both types of 2D electron systems. However, in distinction from a conventional semiconductor 2D electron layer, the plasmon "inertia" in massless graphene is determined by a fictitious "relativistic" effective mass $m_F=E_F/V_F$, where E_F is the Fermi energy.[9,11] Because of that, the plasmon frequency in massless graphene is proportional to $N_s^{1/4}$, where N_s is the sheet electron density whereas in conventional 2D electron systems, the plasmon frequency is proportional to $N_s^{1/2}$. In intrinsic undoped graphene, plasma waves can exist only due to thermionic generation[8,10] or photogeneration[11,13] of free carriers in graphene.

When graphene is patterned into narrow ribbons, the carriers are confined in quasi-one-dimensional (1D) graphene nanoribbons (GNRs).[14–21] Although the band structure of a GNR differs for different, either armchair or zigzag common types of the GNR,[21] a common feature of the GNR is an energy gap opened due to carrier confinement. This band gap can be easily estimated for a relatively wide GNR under a hard-wall boundary condition. In this idealized case, the energy spectrum is

$$E=\pm V_F\sqrt{p_\parallel^2+n^2\left(\frac{\pi\hbar}{w}\right)^2}=\pm\frac{\Delta}{2}\sqrt{n^2+\frac{2p_\parallel^2}{m^*\Delta}}, \quad (1)$$

where $p_\parallel$ is the electron (hole) momentum along the GNR and w is the GNR width, $\Delta=2\pi V_F\hbar/w$ is the energy gap between the conduction and valence bands, $m^*=\Delta/2V_F^2$ is the effective mass, and $n=1,2,3,\ldots$ is the index of 1D subband in the GNR. Near the bottom of the conduction band and the top of the valence band ($n=1$), the spectrum given by Eq. (1) is virtually quadratic $E=\pm(\Delta/2+p_\parallel^2/2m^*)$. For $V_F\approx 10^8$ cm/s^2, formula $\Delta=2\pi V_F\hbar/w$ reasonably well describes the experimental observations of $\Delta=(300-30)$ meV for GNR with the width of 15–90 nm.[19] Those energy-band values correspond to the effective electron masses $(0.01-0.002)m_0$, where m_0 is the free-electron mass. For narrower GNR with the width of nanometer order, this simple model yields $m^*=0.1m_0$, which is very close to the effective mass of zigzag GNR calculated in a first-principles approach.[21] Due to parabolic carrier energy spectrum in GNR, the plasmon dispersion in isolated doped GNR (Ref. 22) is similar to the dispersion of 1D plasmons in semiconductor nanowires,[23]

$$\omega_p=\sqrt{\frac{2e^2N_{1D}}{\varepsilon m^*}q_\parallel|\ln(q_\parallel w)|}$$

in the long-wavelength ($qw\to 0$) quasielectrostatic limit, where ω_p and $q_\parallel$ are the plasmon frequency and wave vector, respectively, ε is the background dielectric constant, e is the electron charge, and N_{1D} is the carrier density per unit length of GNR.

Plasmons in GNRs, like plasmons in semiconductor nanowires,[24] could be observed in optical experiments. A pertinent structure in this case could be a periodic array of GNR enhancing coupling between plasmons in GNR and electromagnetic field. In this paper, we consider plasmons in a 1D dense array of doped (or gated) GNR. We show that the plasmon dispersion in such a system has a 2D plasmon form but the plasmon frequency depends on the angle between the plasmon wave vector and GNR with reducing the plasmon frequency by an order of magnitude and more at oblique angles.

Due to spatial confinement of carriers in GNRs, the macroscopic current in GNR array can flow only in the GNR direction (Fig. 1). In actual experimental case, the plasmon wavelength is dictated by the sample length, which is typically much longer than the period of GNR array and the width of GNR. In this case, the GNR array can be considered

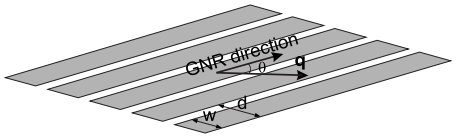

FIG. 1. Schematic of a graphene nanoribbon array.

as a homogeneous 2D plane with anisotropic sheet conductivity. Choosing the Cartesian coordinate system with x-coordinate axis directed along the plasmon wave vector, the sheet conductivity, $\hat{\sigma}$, of such dense GNR array can be described by a tensor,

$$\hat{\sigma} = \sigma \begin{pmatrix} \cos^2\theta & \cos\theta \sin\theta \\ \cos\theta \sin\theta & \sin^2\theta \end{pmatrix}, \tag{2}$$

where θ is the angle between the plasmon wave vector and the GNR direction and

$$\sigma = i\frac{e^2 N_{2D}}{m^*(\omega + i\nu)} \tag{3}$$

is the Drude-type conductivity of the GNR array subject to the oscillating electric field $E\exp(-i\omega t)$ with ν being the electron momentum relaxation rate in the GNR array. The sheet electron density in the GNR array is $N_{2D}=N_{1D}/d$, where N_{1D} is the 1D electron density in each GNR and d is the period of the GNR array. It should be noted that due to the energy-gap inherent in GNR (typically $\Delta > 30$ meV), the plasmons in the GNR array are not subject to interband absorption ($\Delta > \hbar\omega_p$) and, hence, the plasmon absorption is determined only by the intraband electron-scattering rate entering Eq. (3).

In a quasielectrostatic approximation, the dispersion relation for plasmons can be obtained by solving the Poisson equation and continuity equation with conventional boundary conditions. One of those boundary conditions requires the continuity of the in-plane electric field component across the plane of the GNR array while the other describes a jump of the normal component of the dielectric displacement vector across the GNR plane by an amount equal to the oscillating sheet-charge density in the plane of the GNR array having tensor conductivity given by Eq. (2). Such approach yields the following dispersion relation for plasmons in the GNR array:

$$\tilde{\omega} = \omega - i\gamma = \sqrt{\frac{2\pi e^2 N_{2D}}{\varepsilon m^*} q\cos^2\theta - \frac{\nu^2}{4}} - i\frac{\nu}{2}, \tag{4}$$

where $\gamma=\nu/2$ is the plasmon relaxation rate due to its dissipation in the GNR array. The spectrum Eq. (4) is similar to that of 2D plasmons in a homogeneous 2D system with the sheet electron density N_{2D}. The plasmon frequency in the GNR array, however, decreases for oblique angles ($\theta \neq 0$) vanishing for $\theta \to \pi/2$ according to the factor of $\cos\theta$. For typical parameters of GNR, $N_{2D}=10^{12}$ cm^{-2} and $m^*=0.002m_0$, formula (4) yields plasmon frequency about 6 THz for $\theta=0$ (which decreases with increasing θ) for the plasmon wavelength about 30 microns.

In a quasielectrostatic approach, the in-plane electric field E_{in} in the plasma wave is directed along the plasmon wave vector (i.e., at angle θ in respect to the nanoribbon direction). The component of the in-plane electric field parallel to the GNR, $E_\parallel = E_{in}\cos\theta$, defines the restoring Coulomb force $eE_\parallel$ for electrons in GNR. Decrease in the restoring Coulomb force accounts for decreasing the plasmon frequency at oblique angles θ. Plasmons become overdamped [this corresponds to a purely imaginary plasmon eigenfrequency $\tilde{\omega}$ in Eq. (4)] when $q < q_c$, where

$$q_c = \frac{1}{8\pi}\frac{\nu\varepsilon}{\sigma_0\cos^2\theta} \tag{5}$$

with $\sigma_0 = e^2 N_{2D}/m^*\nu$.

It is worth mentioning that in the lossless or ballistic limit ($\nu \to 0$), Eq. (3) can be obtained considering the plasmon dispersion in 1D superlattice of semiconductor nanowires, which in the long-wavelength quasielectrostatic limit is[23]

$$\omega_p = \sqrt{\frac{2e^2 N_{1D}}{\varepsilon m^*} q_\parallel} \times \left[K_0(q_\parallel w) + 2\sum_{n=1}^{\infty} K_0(nq_\parallel d)\cos(q_\perp nd) \right]^{1/2}, \tag{6}$$

where $q_\parallel$ is the plasmon wave vector along the nanowire, $q_\perp$ is the reduced band wave vector defining the plasmon band in 1D array $0 \le q_\perp \le \pi d$, and $K_0(x)$ is the zeroth-order modified Bessel function of the second kind. In a dense GNR array ($q_\parallel d \ll 1$ and $q_\perp \ll \pi/d$), one has[25]

$$\sum_{n=1}^{\infty} K_0(nq_\parallel d)\cos(q_\perp nd) \approx \frac{\pi}{q_\parallel d\sqrt{1+(q_\perp/q_\parallel)^2}} \gg K_0(qw).$$

Then, after introducing notations $N_{2D}=N_{1D}/d$, $\theta = \tan^{-1}(q_\perp/q_\parallel)$, and $q=(q_\parallel^2+q_\perp^2)^{1/2}$, the plasmon spectrum Eq. (6) acquires the form

$$\omega_p = \cos\theta\sqrt{\frac{2\pi e^2 N_{2D}}{\varepsilon m^*} q},$$

which coincides with Eq. (4) for $\nu=0$.

Figures 2 and 3 demonstrate the oblique plasmon frequencies and decay rates as functions of the plasmon wave vector for two different electron relaxation rates corresponding to different electron mobilities in GNR specified in the captions to Figs. 2 and 3. The cutoff plasmon wave vector q_c corresponds to the zero-frequency point of a dispersion curve $\omega(q)$. It is seen in Fig. 2 that the frequency of plasmons with the wavelength longer than ten microns can be tuned from 1 to 10 THz by changing the plasmon propagation angle θ. Experimentally, such plasmons could be excited in GNR arrays with tens-of-micron area by incident terahertz radiation with the electric field polarized in the plane of the GNR array. The plasmon frequency can be varied by changing the polarization of the electric field in incident terahertz wave in respect to the GNR direction. It is worth noting that, in distinction from semiconducting nanowires, the electron effective mass in GNRs essentially depends on the nanoribbon width, exhibiting very small electron effective mass m^*

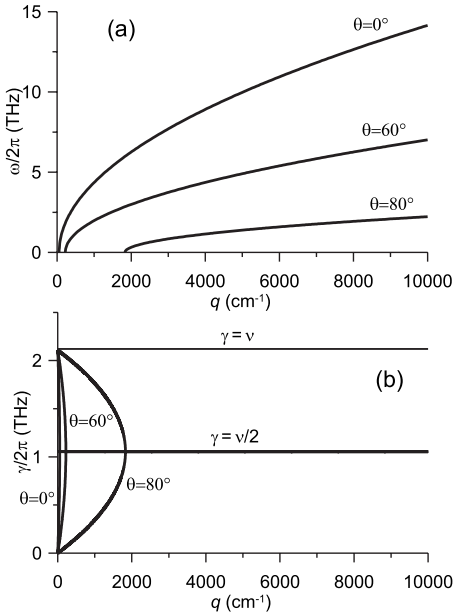

FIG. 2. (a) Plasmon dispersion $\omega/2\pi$ and (b) decay rate $\gamma/2\pi$ as a function of the plasmon wave vector for different values of angle θ and $\nu=1.32\times10^{13}$ s^{-1} (electron mobility is 66 000 cm^2/V s). Parameters of the GNR array are as follows: $m^*=0.002m_0$ and $N_{2D}=10^{12}$ cm^{-2}.

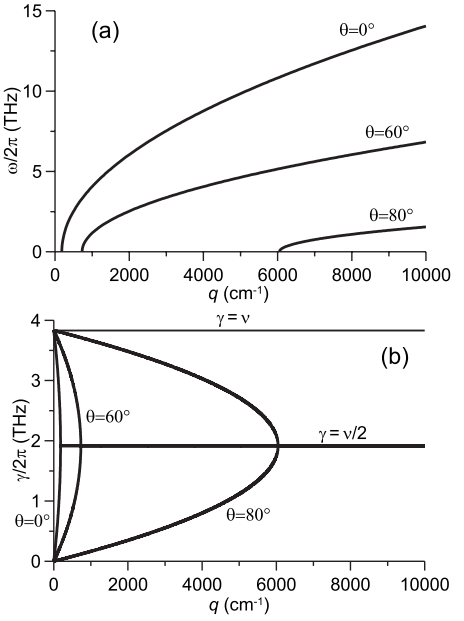

FIG. 3. The same as in Fig. 2 for $\nu=2.4\times10^{13}$ s^{-1} (electron mobility is 36 000 cm^2/V s).

$<0.002m_0$ for GNRs of width about 100 nm and wider. Small electron effective mass in GNRs determines high-terahertz plasmon frequencies with wide range of their variation in GNR arrays.

Nonzero electron concentration in the conduction band (or holes in the valence band) can be also achieved in intrinsic (undoped) graphene in gated graphene structures by applying gate voltage. The plasmon dispersion in the gated GNR array is

$$\tilde{\omega}=\omega-i\gamma=\sqrt{\frac{4\pi e^2N_{2D}}{\varepsilon m^*}\frac{q\cos^2\theta}{1+\coth(qH)}-\frac{\nu^2}{4}}-i\frac{\nu}{2}, \quad (7)$$

where H is the spacing between the array and perfectly conductive gate plate. For short-wavelength plasmons, $qH\gg1$, plasmon dispersion Eq. (7) coincides with that for ungated plasmons given by Eq. (4). For long-wavelength plasmons, $qH\ll1$, Eq. (7) becomes

$$\tilde{\omega}=\omega-i\gamma=\sqrt{\frac{4\pi e^2N_{2D}H}{\varepsilon m^*}q^2\cos^2\theta-\frac{\nu^2}{4}}-i\frac{\nu}{2}$$

yielding the following expression for the plasmon cutoff wave vector of the gated plasmons in the GNR array:

$$\bar{q}_c=\frac{1}{4\cos\theta}\sqrt{\frac{\nu\varepsilon}{\pi\sigma_0H}}. \quad (8)$$

Comparing Eqs. (5) and (8), one obtains $q_c/\bar{q}_c=(2q_cH)^{1/2}<1$, which means that the gated plasmons have higher-cutoff wave vectors.

In conclusion, we have shown that the plasmon frequency in a dense GNR array can reach terahertz range for relatively long plasmon wavelength comparable with terahertz wavelength. The frequency of plasmons in GNR array excited by incoming polarized terahertz radiation can be tuned through the entire terahertz frequency band by changing the angle between the plasmon wave vector and the GNR direction.

This work has been supported by the Russian Foundation for Basic Research through Grants No. 09-02-00395 and No. 08-02-92497 and by the Russian Academy of Science Program "Fundamentals of Nanotechnology and Nanomaterials." The work at Tohoku University and University of Aizu was supported by the Japan Science and Technology Agency, CREST and the Japan Society for Promotion of Science, Japan.

[1] K. Novoselov, A. Geim, S. Morozov, D. Jiang, Y. Zhang, S. Dubonos, I. Grigorieva, and A. Firsov, Science **306**, 666 (2004).
[2] K. Novoselov, A. Geim, S. Morozov, D. Jiang, Y. Zhang, S. Dubonos, I. Grigorieva, and A. Firsov, Nature (London) **438**, 197 (2005).
[3] Y. Zhang, Y.-W. Tan, H. Stormer, and P. Kim, Nature (London) **438**, 201 (2005).
[4] M. Katsnelson, Mater. Today **10**, 20 (2007).

[5] A. Geim and K. Novoselov, Nature Mater. **6**, 183 (2007).
[6] V. Ryzhii, Jpn. J. Appl. Phys. **45**, L923 (2006).
[7] B. Wunsch, T. Stauber, F. Sols, and F. Guinea, New J. Phys. **8**, 318 (2006).
[8] O. Vafek, Phys. Rev. Lett. **97**, 266406 (2006).
[9] E. H. Hwang and S. Das Sarma, Phys. Rev. B **75**, 205418 (2007).
[10] L. Falkovsky and A. Varlamov, Eur. Phys. J. B **56**, 281 (2007).
[11] V. Ryzhii, A. Satou, and T. Otsuji, J. Appl. Phys. **101**, 024509 (2007).
[12] V. Popov, O. Polischuk, and M. Shur, J. Appl. Phys. **98**, 033510 (2005).
[13] F. Rana, IEEE Trans. Nanotechnol. **7**, 91 (2008).
[14] C. Berger, Z. Song, X. Li, X. Wu, N. Brown, C. Naud, D. Mayou, T. Li, J. Hass, A. Marchenkov *et al.*, Science **312**, 1191 (2006).
[15] Y.-W. Son, M. L. Cohen, and S. G. Louie, Phys. Rev. Lett. **97**, 216803 (2006).
[16] Y.-W. Son, M. L. Cohen, and S. G. Louie, Nature (London) **444**, 347 (2006).
[17] K. Wakabayashi, Phys. Rev. B **64**, 125428 (2001).
[18] V. Barone, O. Hod, and G. E. Scuseria, Nano Lett. **6**, 2748 (2006).
[19] M. Y. Han, B. Ozyilmaz, Y. Zhang, and P. Kim, Phys. Rev. Lett. **98**, 206805 (2007).
[20] Z. Chen, Y.-M. Lin, M. Rooks, and P. Avouris, Physica E **40**, 228 (2007).
[21] L. Yang, C.-H. Park, Y.-W. Son, M. L. Cohen, and S. G. Louie, Phys. Rev. Lett. **99**, 186801 (2007).
[22] L. Brey and H. A. Fertig, Phys. Rev. B **75**, 125434 (2007).
[23] S. Das Sarma and W. Y. Lai, Phys. Rev. B **32**, 1401 (1985).
[24] T. Demel, D. Heitmann, P. Grambow, and K. Ploog, Phys. Rev. Lett. **66**, 2657 (1991).
[25] I. S. Gradshteyn and I. M. Ryzhik, *Table of Integrals, Series, and Products* (Academic, New York, 1996), p. 992, Eq. 8.526.